ANALYSIS OF TORNADO EVENTS IN ALABAMA USING GEOSPATIAL TECHNIQUES: IMPACTS AND AGGRAVATING FACTORS

by

Navya Kolli

Submitted in partial fulfillment of the
requirements for Departmental Honors in
the Department of Geological Sciences
Texas Christian University
Fort Worth, Texas

May 2, 2022

ANALYSIS OF TORNADO EVENTS IN ALABAMA USING GEOSPATIAL TECHNIQUES: IMPACTS AND AGGRAVATING FACTORS

Project Approved:

Supervising Professor: Esayas Gebremichael, Ph.D.
Department of Geological Sciences
Omar Harvey, Ph.D.
Department of Geological Sciences
Grant Ferguson, Ph.D.
Department of Political Science

ABSTRACT

In this research project, geospatial data was used to map the spatial distribution of tornado events in Alabama and compare the relationship between the intensity of the events and elevation. In addition, how land surface modification have amplified the effect of the tornadoes was assessed closely. The analysis showed: (1) remote sensing technology was able to capture the spatial distribution of the tornado tracks much better than ground-based observations; (2) higher elevations experience more intense tornado damage, and (3) change in land cover, specifically due to anthropogenic activity, amplifies tornado damage.

TABLE OF CONTENTS

CHAPTER I: Background

1.1 Introduction

Tornadoes are defined as rotating columns of air touching the ground (National Weather Service (NWS), 2022). The intensity of the damage occurring from tornadoes is measured using the Enhanced Fujita (EF) Scale (Table 1) and is used to assign a tornado a 'rating' based on estimated wind speeds and related damage (Strader et al., 2014). Tornadoes with the highest wind speed and that cause severe destruction are classified as EF5 while those that cause the least damage and have the lowest wind speed are classified as EF0 (Table 1).

Category	Wind-Gust (m/s)	Typical Damage
EF0	29-38	Large tree branches broken; Trees may be uprooted; Strip mall roofs begin to uplift
EF1	38-49	Tree trunks snap; Windows in Institutional buildings break; Facade begins to tear off
EF2	49-60	Trees debark; Wooden transmission line towers break; Family residence buildings severely damaged and shift off foundation
EF3	60-74	Metal truss transmission towers collapse; Outside and most inside walls of family residence buildings collapse
EF4	74-89	Severe damage to institutional building structures; All family residence walls collapse
EF5	>89	Severe general destruction

Table 1. Tornado categories based on wind speed and damage (NWS, 2022)

Although no single area is immune to tornadoes, they are more common in the United States than in any other country, with most tornadoes occurring east of the Rocky Mountains, most prominently in an area called Tornado Alley in the Midwest. Tornado Alley is the most widely known area for recurrent tornado occurrences but there is another area that has a high frequency of strong, long-track tornadoes that move at higher speed. This area is known as the Dixie Alley and stretches from East Texas into western North Carolina, with the heart of the Dixie Alley located in Alabama and Georgia (Bradburn, 2016). Many prominent tornado outbreaks have occurred in this region, which is the focus of this paper, specifically in the state of Alabama.

The state of Alabama is located in the southeastern United States (Figure 1) and has experienced its share of strong tornadoes, leading with the state of Oklahoma in terms of the highest number of EF5 tornadoes with eight since 1950 (NWS, 2022). Given the severity of the tornadoes in the state, it would be helpful to analyze the tornado tracks, their impact, and factors that affect their severity more closely.

1.2 Study Sites

In order to better understand the patterns of tornadoes in Alabama, two specific case study areas were chosen as test sites in this study (Figure 1). These areas were chosen because they have experienced recurring events that have data allowing for a closer analysis and comparison of events. Two major tornado events were chosen for both case study areas that were of an overall EF value of at least 3 or higher. The reason certain events were chosen will be explained further in Section 2.1.

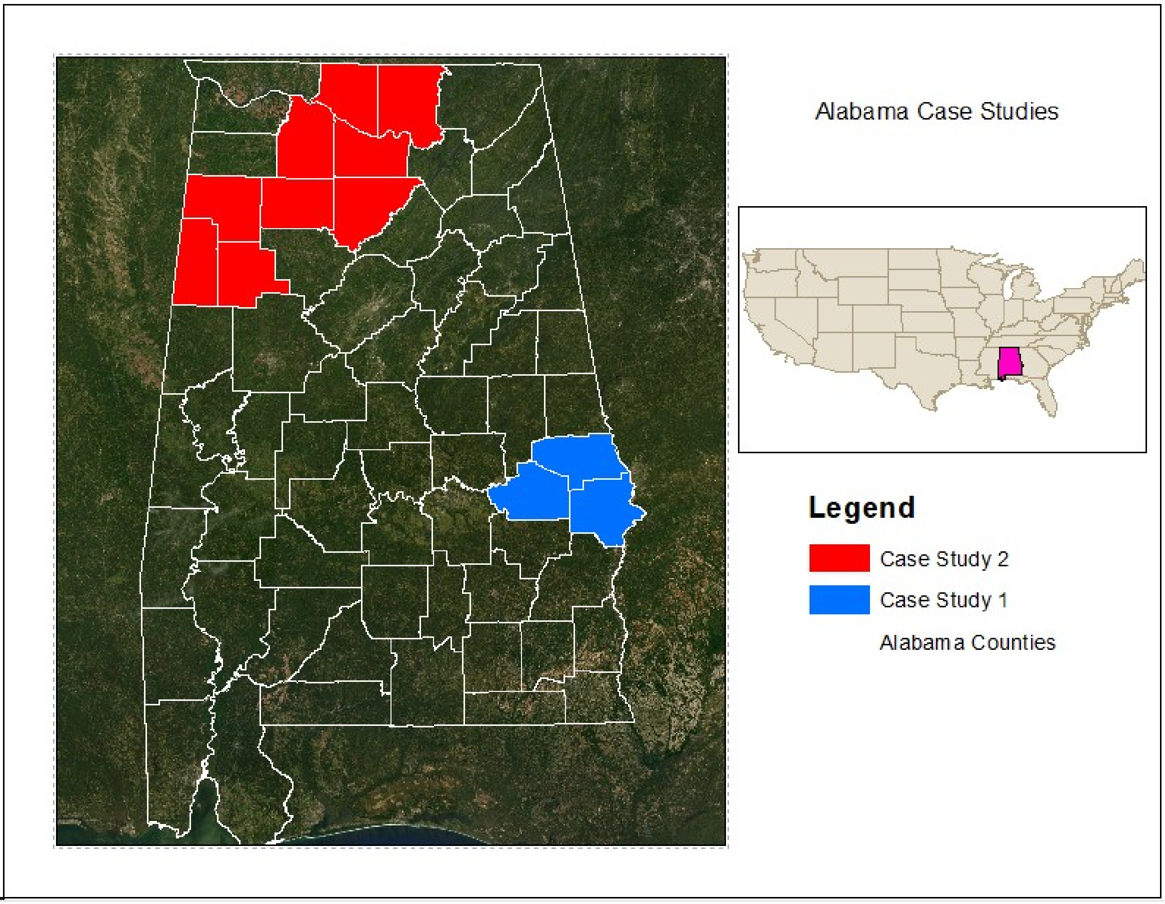

Figure 1. Case study sites in Alabama State

The areas explored in case study 1 encompass several counties close to the eastern edge of central Alabama located in and around the city of Auburn (Figure 1). The first event chosen in this study occurred on April 29, 2014. This EF3 tornado was part of a widespread tornado outbreak occurring in the central and southern United States. It had a track length of 31 miles passing through several counties and destroying more than 300 homes and businesses in the area. The second event occurred roughly 5 years later on March 3, 2019 and was much more damaging to the area as a prominent EF4 tornado, resulting in dozens of deaths as well (NWS, 2022). Case study 2 is concerned with several counties in north Alabama, which includes the largest municipality in the state, Huntsville. The first major tornado event in this area with readily available data occurred on April 3, 1974 and was known as the 1974 Palm Sunday Super Outbreak. It was the largest tornado outbreak on record for a single 24-hour period at the time causing major destruction and death. This outbreak became second to the next tornado event in the case study, which occurred on April 27, 2011. These events are incredibly similar in that they both have parallel tracks and are EF5 tornadoes decimating the same region and deserve a closer look.

1.3 Literature Review

There are several ways of mapping tornado impacts. The first method is in-situ (direct) measurements of tornado winds and damage assessment. These measurements can be obtained using land-based sensors or through in-person field monitoring. Such measurements are extremely rare, difficult, and dangerous to obtain because of the damaging and unpredictable nature of tornadoes and limitations on predicting instances of tornadoes and their paths (Fleming et al., 2013; Karstens et wal., 2013; Kosiba & Wurman, 2013). Direct measurement of tornado winds using the land-based sensors are further complicated by the inability of radar systems to measure the tornado winds near the ground surface, the location that most often impacts buildings and structures of that nature (Wurman et al., 2013). Direct measurements also have limited spatial coverage, as the area that can be mapped/assessed using the in-situ observations is limited. Due to all of these drawbacks of the direct measurements, another technique called remote sensing has emerged as a safer and detailed (observation) alternative to in-situ measurements. Remote sensing is the acquisition of information about an object or phenomenon without making physical contact with the object (Womble et al., 2018). Today, remote sensing and geospatial technologies have played a crucial role in monitoring and analyzing tornado outbreaks. In comparison to in-situ observations, it is safer, and the data is more readily available. It also provides a wide-scale view of the event. Through remote sensing, we have gained insight into estimated tornado wind speeds based on the intensity of the damage, the tornado track, etc.

Remote sensing data can be analyzed in a Geographic Information Systems (GIS) environment, which is specifically a type of database containing geographic data, combined with software tools for managing, analyzing, and visualizing the data (Strader et al., 2014). In regard to tornadoes, these procedures have resulted in spatially referenced tornado damage survey information for an increasing number of significant and violent events (Strader et al. 2014). As a result, tornado track data and any other necessary geographic data is readily available to the public for use in data analysis and interpretation.

The mode of acquisition of the remote sensing datasets used for impact assessments can be broadly classified as passive and active systems depending on the source of electromagnetic energy that the systems use to observe the Earth's surface. Passive systems rely on the electromagnetic energy emitted from the sun and reflected back from the surface. Imagery acquired by such systems is heavily affected by clouds (Womble et al., 2018). These include the pioneer earth observation satellite mission called the Landsat mission. The mission is one of the earliest and longest-running earth programs utilizing passive sensors that can collect energy from the multiple components/ranges of wavelengths of the electromagnetic energy (called bands), and most have a revisit time of 16 days with most bands having a resolution of 30 m (United States Geological Survey (USGS), 2020; table 2). The Landsat missions (1,2,3,4,5,7,8, and 9) have been providing open-access earth observation since the mid-1970s, allowing for monitoring occurring from then all the way into the present day (Song et al., 2021).

Mission	Bands	Wavelength (micrometers)	Resolution (meters)
Landsat 1-3	Band 4	0.5-0.6	60
	Band 5	0.6-0.7	60
	Band 6	0.7-0.8	60
	Band 7	0.8-1.1	60
Landsat 4 – 5 (Thematic Mapper)	Band 1	0.45-0.52	30
	Band 2	0.52-0.60	30
	Band 3	0.63-0.69	30
	Band 4	0.76-0.90	30
	Band 5	1.55-1.75	30
	Band 6	10.40-12.50	30
	Band 7	2.08-2.35	30
Landsat 8 (Enhanced Thematic Mapper)	Band 1- Coastal Aerosol	0.43-0.45	30
	Band 2- Blue	0.45-0.51	30
	Band 3- Green	0.53-0.59	30
	Band 4- Red	0.64-0.67	30
	Band 5- Near Infrared (NIR)	0.85-0.88	30
	Band 6- SWIR 1	1.57-1.65	30
	Band 7- SWIR 2	2.11-2.29	30
	Band 8- Panchromatic	0.50-0.68	15
	Band 9- Cirrus	1.36-1.38	30
	Band 10- Thermal Infrared (TIRS) 1	10.60-11.19	100
	Band 11- Thermal Infrared (TIRS) 2	11.50-12.51	100

Table 2. Bands and spatial resolutions of satellites of the Landsat mission (USGS, 2020)

Another passive satellite utilized in tornado studies is the two-satellite constellation Sentinel-2 (Table 3) that is operated by the European Space Agency (ESA), with a revisit time of 5-10 days and a spatial resolution of 10 m (Isip et al., 2020). Combined, imaging taken from these satellites allow for a wide range of time to be covered as efficiently as possible and allows for an in-depth and comprehensive analysis.

Bands	Central Wavelength (µm)	Resolution (m)
Band 1- Coastal Aerosol	0.443	60
Band 2- Blue	0.490	10
Band 3- Green	0.560	10
Band 4- Red	0.665	10
Band 5- Vegetation Red Edge	0.705	20
Band 6- Vegetation Red Edge	0.740	20
Band 7- Vegetation Red Edge	0.783	20
Band 8- NIR	0.842	10
Band 8A- Vegetation Red Edge	0.865	20
Band 9- Water Vapor	0.945	60
Band 10- Cirrus	1.375	60
Band 11- SWIR	1.610	20
Band 12- SWIR	2.190	20

Table 3. Bands and spatial resolutions of the Sentinel-2 satellite (ESA, 2022)

Active sensors, which are utilized in many tornado studies as well, generate their own source of electromagnetic energy, and as a result are able to observe the surface regardless of solar illumination availability. Weather conditions are not as much of a factor in obtaining imaging when using active sensors as they can penetrate through dense cloud covers. This property makes the datasets preferable following tornado events where dense cloud cover could hinder the observation of the impact. Synthetic aperture radar data (SAR) are one such datasets acquired by active systems/satellites (Kumar et al., 2021). SAR datasets can be used to delineate the extents of tornado tracks particularly in areas that cannot be easily accessed (Womble et al., 2018). SAR datasets acquired by the Sentinel-1 mission are currently the only SAR datasets that are made available to the public free of charge. Similar to the Sentinel-2 mission, the Sentinel-1 mission is a two-satellite constellation and the revisit time (over the same area) is 6-12 days (Kellndorfer et al., 2022).

Several studies used multi-source datasets to access the factors that affect the intensity of tornado impact (damage). For example, a study on the temporal and spatial relationship of a tornado outbreak in Central Alabama revealed that there is some correlation between elevation and tornado intensity, and that the majority of the heaviest damage occurred in relatively lower elevations (Flynn & Islam, 2018). But this study was based on the assessment of a single event and the accuracy of the analysis should be supported with data from multiple events. A study on the relationship between land use/land cover changes and tornado impact found that an increase in tornado damage is associated with land cover changes (Strader et al., 2014). These possible relationships between elevation and land cover change with tornado intensity will further be explored in this paper using datasets from multiple case studies.

1.4 Objectives

Many tornado events occurred between 1974 and the present day in the state of Alabama. A few of the most prominent events in the two case study sites (Figure 1) were chosen to analyze more closely. In this study, the following objectives are explored: 1) storm paths will be mapped using data acquired by passive and active satellites that can be used as potential replacements to time-consuming and at times not safe ground-based damage assessments; 2) investigate the relationship between land cover changes and tornado impact intensity; and 3) assess the relationship between surface elevation and severity of a tornado impact.

For both of the case study areas, two major tornado events were chosen that were of an overall EF value of at least 3 or higher. The two events of each case study had a gap in time of at least 5 years, and the tracks overlapped and/or were parallel to each other. A gap between the events ensures that structures are rebuilt, and other such indicators will not overlap or skew results in regard to land cover assessment. The two tracks chosen for each case study followed similar paths in that in case study 1, the tornadoes moved from west to east, going over Auburn and into counties in the neighboring state of Georgia such as Macon County (Figure 1). In case study 2, the tornadoes moved from the southwest to the northeast, passing through the city of Huntsville or areas near to it (Figure 1). These steps were taken in order to have a clearer understanding of the relationship between land cover, elevation, and EF values from a spatial and temporal sense. Specifically, the aim is to fully analyze data collected over a specific area (spatial) and a certain time period (temporal).

Chapter II: Data and Methods

2.1 Datasets

In order to complete the above-stated objectives, several programs and datasets were used (table 4). One of the main programs used was ArcMap, which is a part of the ESRI ArcGIS suite and allows for geospatial data to be viewed, edited, and analyzed by users of the program. Other programs utilized were ArcGIS Pro and Google Earth Engine. Remote sensing datasets used in this study include Sentinel-1, Sentinel-2, and Landsat. Ground-based tornado impact datasets (EF-values) for the investigated events were obtained from the NWS and National Oceanic and Atmospheric Administration (NOAA).

Active Satellite Data	**Passive Satellite Data**	**In-situ**
• Sentinel-1 • DEM	• Landsat • Sentinel-2	• EF-values

Table 4. Datasets used in the study

2.2 Methods

In Case Study 1 two major events were analyzed: the April 29, 2014, and March 3, 2019. These events are a mere five years apart but were chosen since they are one of the few major tornadoes to occur in the same area and have parallel tracks. Data was also more easily accessible, allowing for a better analysis. For Case Study 2, the tornadoes events chosen occurred on April 3-4, 1974, and April 27, 2011. These events were chosen for the same reasons as those events that were selected for investigation in Case Study 1. However, an added factor to consider includes a significant increase in urban areas due to the longer period of time between the two tornado events. This will likely show that more of what used to be forested/vegetated lands in 1974 are now urban areas or are turning to bare land due to deforestation and as a result, this may cause more damage by comparison. This will be further analyzed in the discussion of the results.

Two methods were used to map the tornado tracks and damage extents. The first method involved importing and isolating the spatial (georeferenced) EF and tornado track data from NWS and NOAA sources to the extents of the study sites. The storm track will be defined based on these datasets. In the absence of geospatial tornado track and EF value data, non-georeferenced digital tornado data were digitized and georeferenced and the tornado track and EF values that fall within the case study sites were extracted from the georeferenced data/maps (Figure 2).

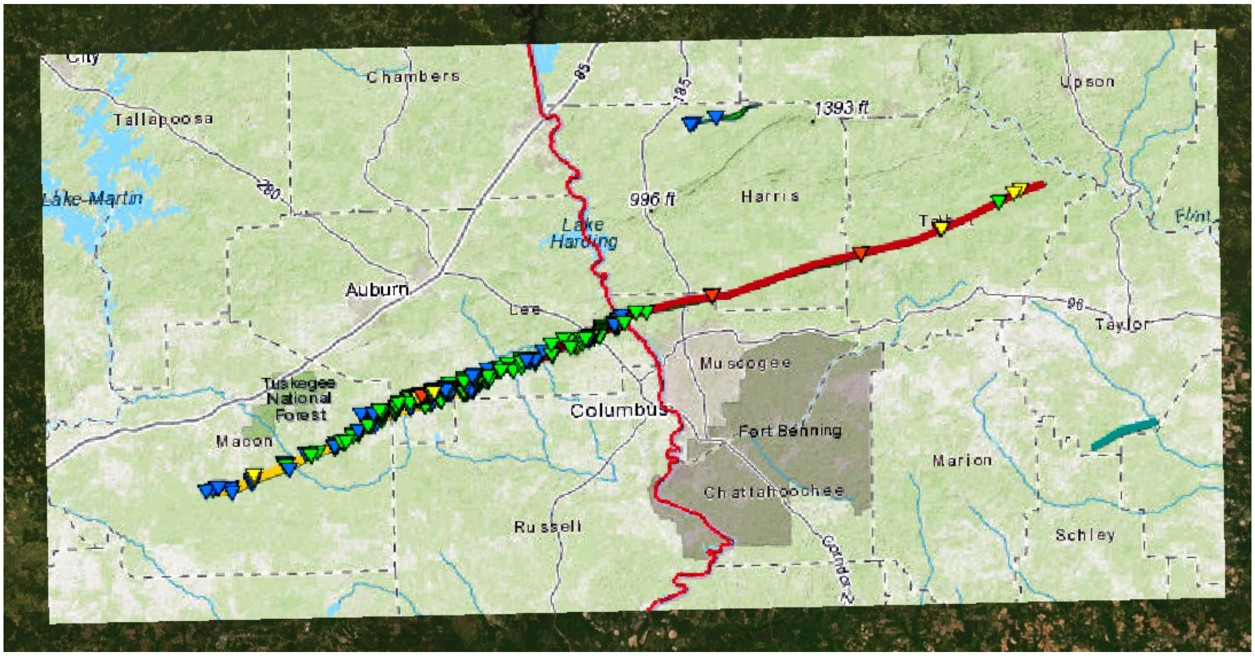

Figure 2. Digitization of JPEG of the 2019 tornado path

To map the full extent of the tornado impact, a supervised classification procedure was applied on Landsat and Sentinel-2 datasets. The imagery before the tornado events were initially classified. The tornado track or sites where the EF values were taken were used as a training sample that were used as inputs for the post-event imagery classification. In most tornado affected areas, an area that was classified as urban land in the pre-event imagery was turned to bare land immediately following in the days after the tornado event. The classified pre-event imagery in the two case studies were correlated with the EF data to see the relationship between land cover change and tornado intensity. For example, the classified pre-event imagery of the 1974 event and its EF values were corresponded with the pre-event imagery and EF-values of the 2011 event. If the area in 1974 was covered by dense forest and the EF value was low and the same area underwent a land cover change (to urban for instance) and resulted in a higher EF value, it indicates that altering the landcover amplifies tornado impact. In order to bolster these results, unsupervised classification was also performed using Google Earth Engine (GEE) (Figure 3). GEE is a cloud-based geospatial processing platform that provide multitude of tools to analyze satellite imagery and geospatial datasets obtained from different sources including Landsat and Sentinel datasets (Mutanga & Kumar, 2019). Unsupervised classifications were quick and helpful to better understand general patterns of land use in an area, but are not as accurate as supervised classifications of the study areas.

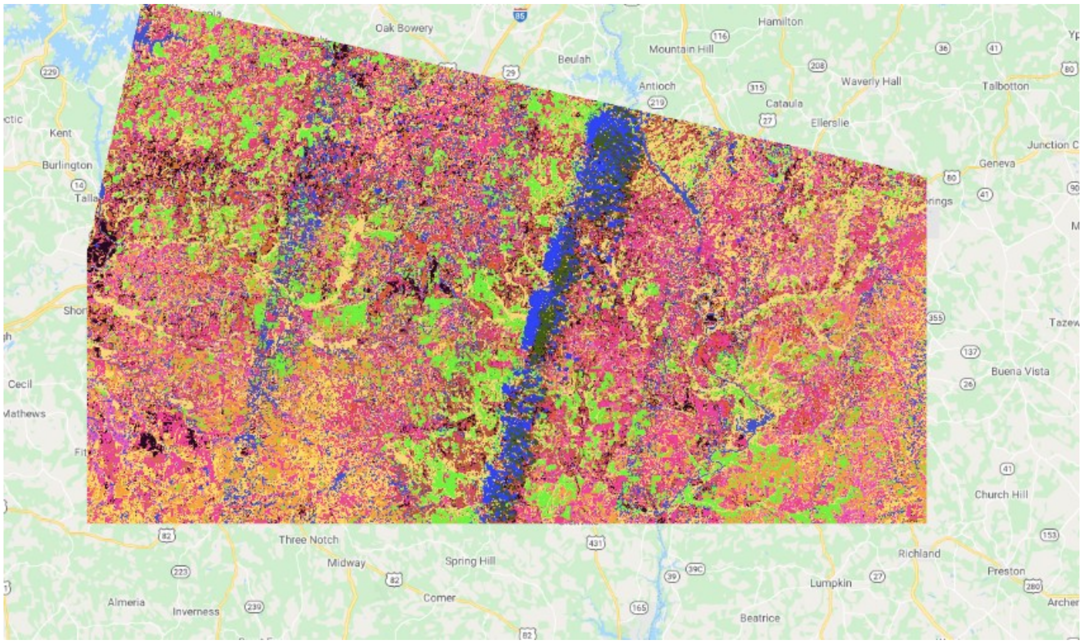

Figure 3. Unsupervised classification performed utilizing GEE

The storm track of each event was also overlaid with a Digital Elevation Model (DEM) of the area that was acquired using the Shuttle Radar Topography Mission (SRTM) in order to observe the relationship between elevation and tornado intensity. Tornado intensity (EF) values and the elevation value at the point where the EF measurement was taken, extracted the SRTM DEM, were compared against each other in search of any patterns or relationships. For example, if an area has a higher DEM value and was affected by a higher EF value, it indicates that increase in elevation amplifies the intensity of tornado damages and areas at higher altitude are vulnerable to the tornado hazard.

Chapter III: Results and Discussion

3.1 Mapping Damage Extent

The damage extents were clearly mapped for most of the tornado paths using Landsat and Sentinel-2 datasets (Figures 4 and 5). The 2014 event from case study 1 was unable to be properly mapped and show a clear distinction between the storm path and surrounding area. This is likely because the 2014 event was an EF3 tornado while the others were an EF4 or EF5. The analysis of the 1974 event from case study 2 revealed a somewhat visible storm path, although it is not as clear as the tornado tracks of the other tornado events. This is likely attributed to the resolution of the imagery. The 1974 imagery was taken using Landsat 1, which has a spatial resolution of 60 meters (Table 2). Imagery taken from later Landsat missions since then have higher spatial resolutions (30 meters). As a result, land cover change is better detected more precisely in the later missions than in the past. This is likely the reason why analysis of the 1974 event did not show a clear tornado track. Overall, the 2011 and 2019 events had the clearest storm paths (Figures 4 and 5) due to their high damage intensity and the high-resolution imagery acquired to perform more accurate supervised classifications.

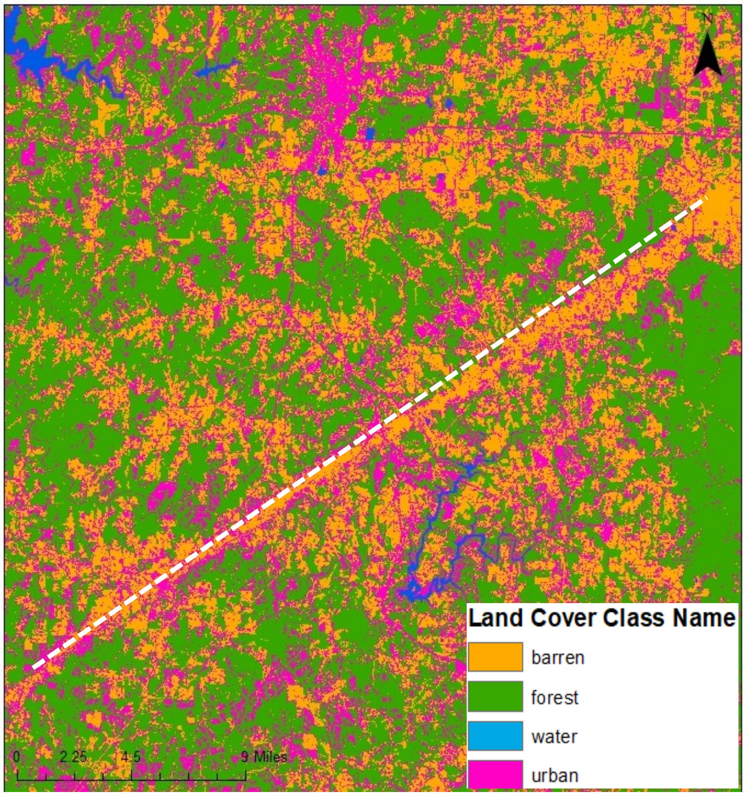

Figure 4. Result of the supervised classification procedure for the 2011 case study. The dashed white line superimposed on the barren land indicates the tornado track.

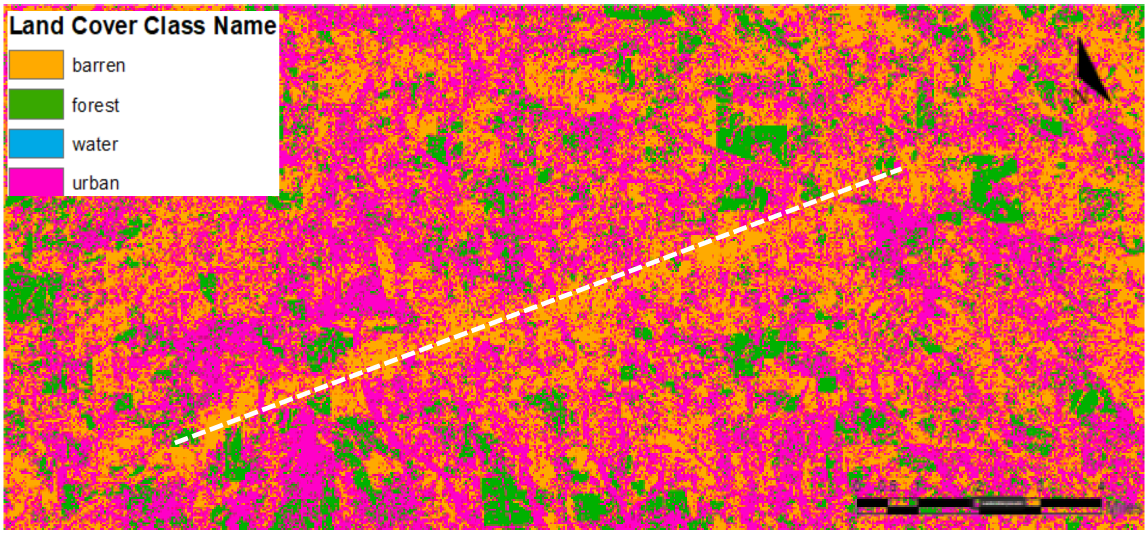

Figure 5. Result of the supervised classification procedure for the 2019 case study. The dashed white line superimposed on the barren land indicates the tornado track.

The imagery to map the damage extents was taken from passive sensors, namely Landsat and Sentinel-2, as stated above. Because of cloud conditions that accompany tornado events, the availability of clear (cloud-free) imagery after tornado events is limited. Cloud-free imagery may become available after extended period of time after the event in some cases. This will make it difficult to determine the tornado track and assess the impact. SAR imagery taken by sensors that can generate their energy and observe the surface regardless of atmospheric conditions will be useful in such cases. Sentinel-1 data was used in this study to demonstrate the capability of the datasets for mapping tornado tracks. Only the 2019 event analyzed since Sentinel-1 SAR datasets are available post 2014 after the launching of the Sentinel-1 mission. The storm path was mapped by applying a change detection assessment on two Sentinel-1 imagery taken before and after the tornado event. The storm path was clearly mapped using this approach for the 2019 case study (Figure 6). This is useful for damage assessment immediately after a tornado event. SAR imagery are made available as a single band gray-scale imagery and hence are not the ideal choice for understanding land use change through supervised classifications.

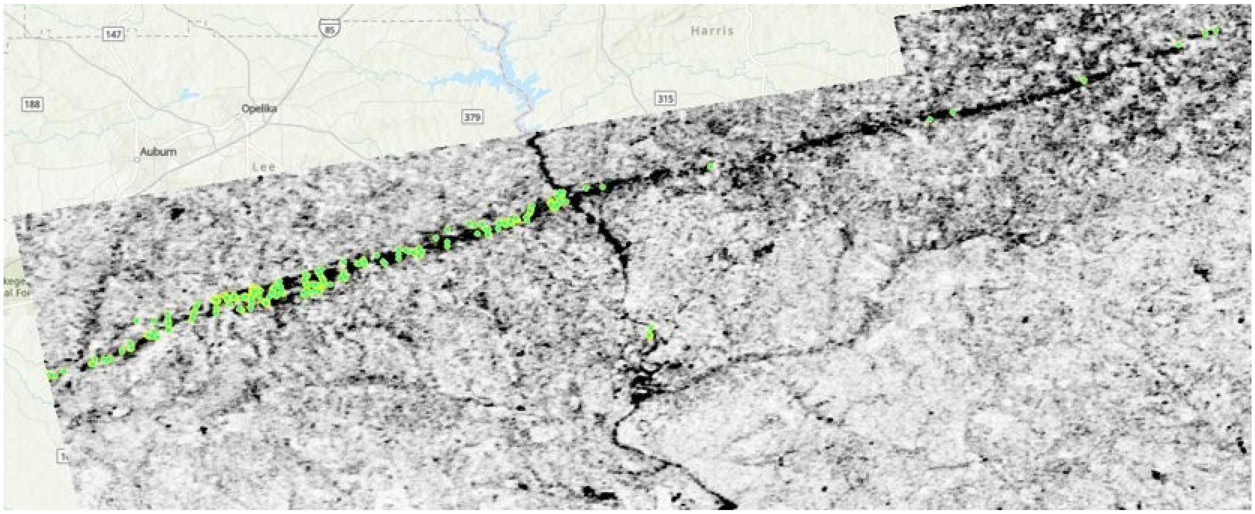

Figure 6. SAR Analysis of the 2019 case study. Tornado tracks are shown as black colors. EF values are overlaid on the SAR result to show the spatial correspondence between the two.

3.2 Land Cover Change vs. Damage Intensity

Land cover change was compared to damage intensity by taking points from two different events in the same case study area and finding the ones from different events that overlapped or that were significantly close to each other. The points were matched up one-to-one manually, with the point from one event being compared to the point closest to it from the other event in the case study. The land cover results generated following the supervised classification procedure were used to get the land cover information of the point where the EF values were obtained. Both EF values and land cover data were compiled on a single table for each of the case studies. Once these points were in the same table, a calculation was performed to measure the difference in EF value between the two points as well as the land cover change (Tables 5 and 6).

Before 2019 Event	Before 2014 Event	EF Difference
Urban	Forest	EF3
Urban	Forest	EF2
Urban	Barren	EF2
Urban	Forest	EF1

Table 5- Case Study 1 Table for Land Cover Change vs Damage Intensity

Before 2011 Event	Before 1974 Event	EF Difference
Urban	Forest	EF3
Urban	Barren	EF2
Urban	Forest	EF2
Barren	Forest	EF1
Barren	Forest	EF1

Table 6- Case Study 2 Table for Land Cover Change vs. Damage Intensity

Following the assessment, areas that overlapped or lying in proximity where a difference in EF values between the events were calculated were included in the tables and figures (Figures 7 and 8; Tables 5 and 6). Overall, these points revealed that there was a significant difference in

EF value between the points. In particular, the areas that changed in land cover from forest or barren land to urban area experienced a higher damage intensity when a tornado came back to the same area later. A few points also experienced a difference in EF value attributed to a decrease in damage intensity over time, but this is due to the forest area being converted into barren land, which cannot have a high EF value since there is little, if any, damage to existing structures in those areas. This is seen in both case studies but is notable in case study 2 (Figure 9). In merely 5 years, a significant amount of forest area was cleared into barren land or/and urbanized as well.

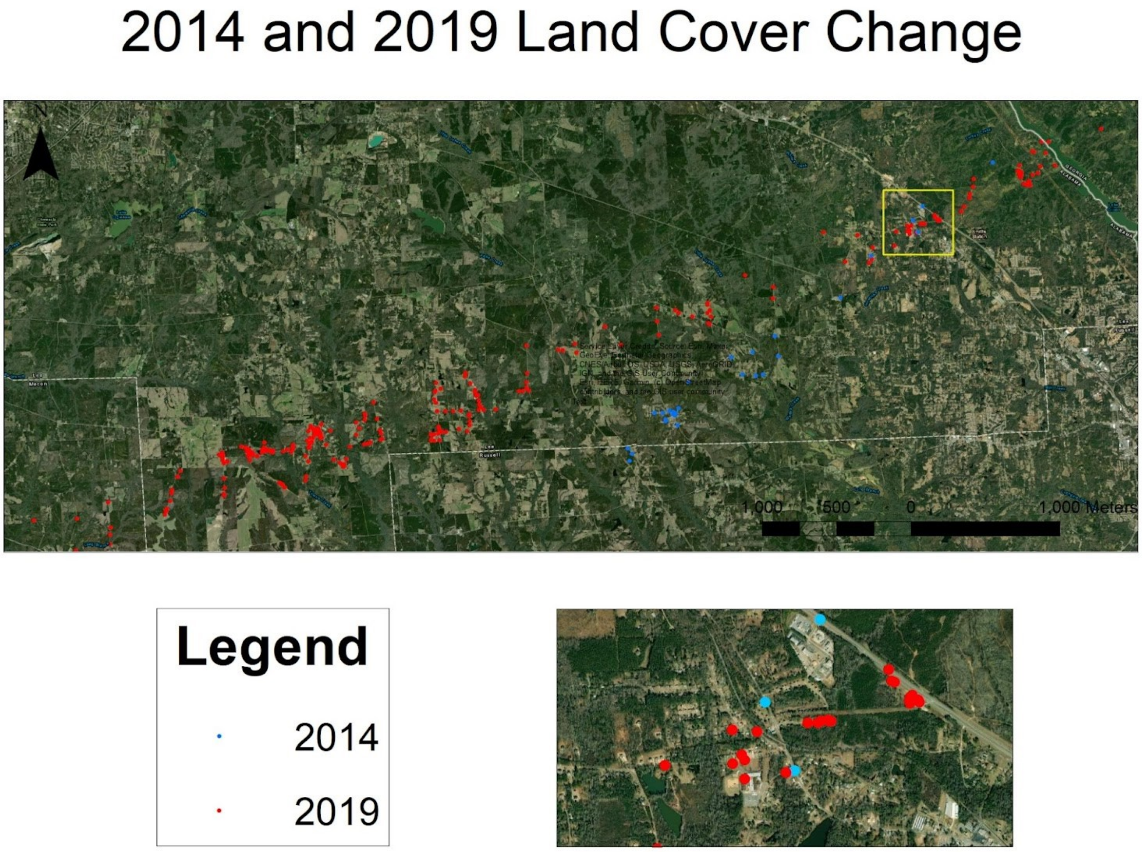

2014 and 2019 Land Cover Change

Figure 7. Land Cover Change vs. Damage Intensity for case study 1

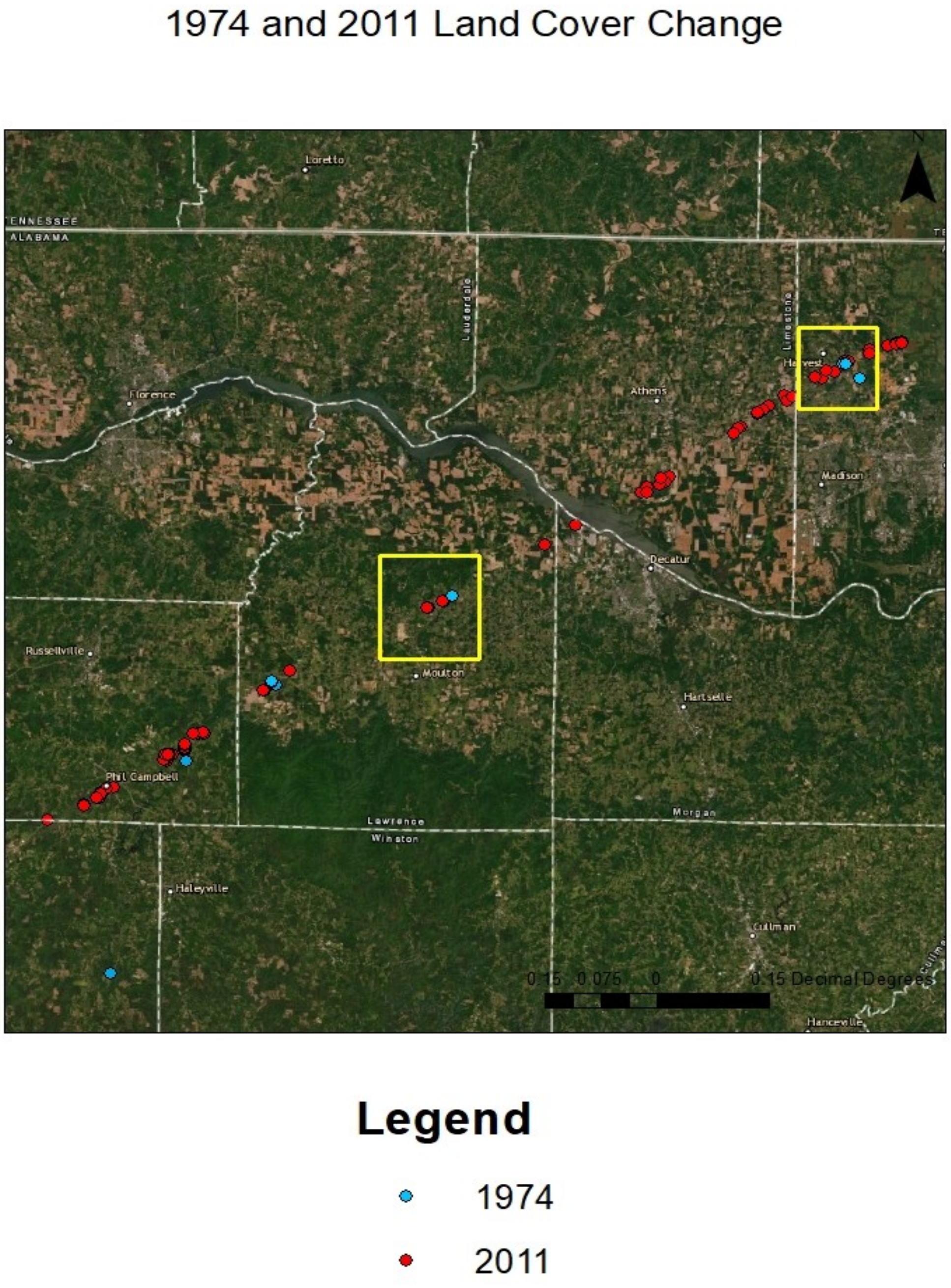

Figure 8. Land Cover Change vs. Damage Intensity for case study 2

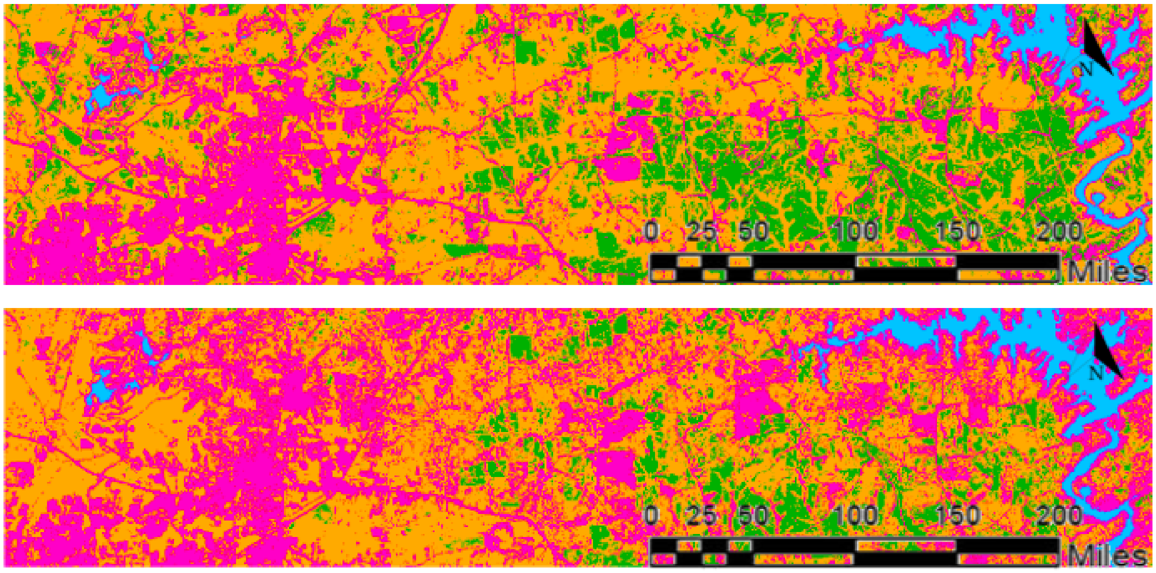

Figure 9. Urban sprawl on outskirts of Auburn-Opelika area (Top: 2014, Bottom: 2019)

3.3 Elevation vs. Damage Intensity

The relationship between elevation and damage intensity was assessed for case study two. Previous studies in case study 1 stated that there exists an inverse relationship between elevation and tornado intensity; that is, areas with lower elevations are affected by higher category tornado (Flynn & Islam, 2018). On the other hand, the analysis in this study for the 2014 and 2019 events (case study 2) showed a direct correlation between elevation and damage intensity (Figure 10). That is, as elevation increases, so does the damage intensity. There were many points with a DEM value of -9999 (error values) that were excluded since they were skewing the data. These points were not of any significance since they are areas without any elevation data.

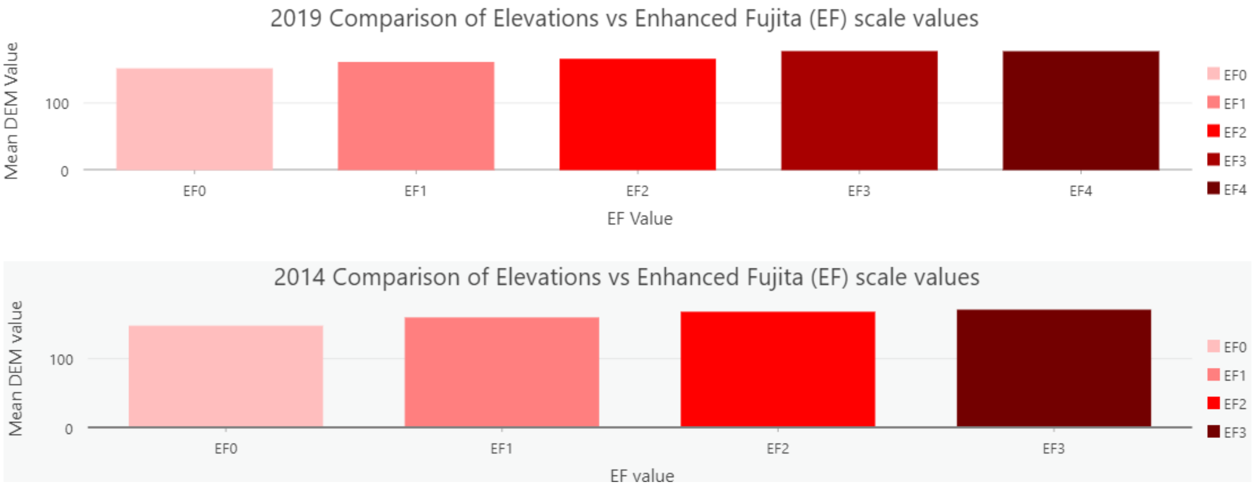
2019 Comparison of Elevations vs Enhanced Fujita (EF) scale values

2014 Comparison of Elevations vs Enhanced Fujita (EF) scale values

Figure 10: Elevation vs. Damage Intensity for case study 2

In the future, this relation between elevation and damage intensity can be taken into consideration when building new structures. A preference may be given to constructing new structures or expanding cities into locations with a lower elevation.

Chapter IV: Conclusion

Two case study areas in Alabama were assessed in this study to map the extent of tornado impacts, and investigate the relationship between land cover change, elevation, and tornado intensity. Remote sensing data acquired by passive and active sensor as well as in-situ data were used for the assessment.

The results show:

- The case studies were able to show a clear storm path for the tornadoes that were EF4 tornadoes or higher, and the damage intensity was able to be mapped.
- Investigation for analyzing the relationship between land cover change and damage intensity revealed that anthropogenic activity (alteration of the land cover such as urbanization) amplifies the tornado damage.
- The analysis of elevation in relation to damage intensity reveals that there is a direct correlation – that is, as elevation increases, damage intensity increases as well.
- Ground-based damage assessments can be replaced with SAR analysis for faster and more efficient results in the immediate aftermath of a tornado. In the future, a combination of active and passive sensors can be used to best assess the impacts of tornado damage in the short-term and the long-term.

References

Burow, D., Herrero, H. V., & Ellis, K. N. (2020). Damage analysis of three long-track tornadoes using high-resolution satellite imagery. Atmosphere, 11(6), 613.

Bradburn, M. (2016). *Tornado Density and Return Periods in the Southeastern United States: Communicating Risk and Vulnerability at the Regional and State Levels* (Doctoral dissertation, East Tennessee State University).

European Space Agency (ESA). (2022). “Radiometric resolutions” Retrieved April 16, 2022, from https://sentinel.esa.int/web/sentinel/user-guides/sentinel-2-msi/resolutions/radiometric.

Fleming, M. R., Haan, F. L., & Sarkar, P. P. (2013). Turbulent structure of tornado boundary layers with translation and surface roughness. In 12th Americas Conf. on Wind Engineering (Seattle, WA).

Flynn, W., & Islam, T. (2018). Spatial and temporal analysis of the 27 April 2011 tornado outbreak in central Alabama. *GeoJournal*, *84*(2), 533–544. https://doi.org/10.1007/s10708-018-9874-3

Isip, M. F., Alberto, R. T., & Biagtan, A. R. (2020). Exploring vegetation indices adequate in detecting twister disease of onion using Sentinel-2 imagery. Spatial Information Research, 28(3), 369-375.

Karstens, C. D., Gallus Jr, W. A., Lee, B. D., & Finley, C. A. (2013). Analysis of tornado-induced tree fall using aerial photography from the Joplin, Missouri, and Tuscaloosa–Birmingham, Alabama, tornadoes of 2011. Journal of Applied Meteorology and Climatology, 52(5), 1049-1068.

Kellndorfer, J., Cartus, O., Lavalle, M., Magnard, C., Milillo, P., Oveisgharan, S., ... & Wegmüller, U. (2022). Global seasonal Sentinel-1 interferometric coherence and backscatter data set. Scientific Data, 9(1), 1-16.

Kosiba, K. A., & Wurman, J. (2013). The three-dimensional structure and evolution of a tornado boundary layer. Weather and Forecasting, 28(6), 1552-1561.

Kumar, R., Rani, S., & Maharana, P. (2021). Assessing the impacts of Amphan cyclone over West Bengal, India: a multi-sensor approach. Environmental monitoring and assessment, 193(5), 1-21.

Mutanga, O., & Kumar, L. (2019). Google earth engine applications. Remote Sensing, 11(5), 591.

National Weather Service (NWS). (2022). Retrieved April 29, 2022, from https://www.weather.gov/

Strader, S. M., Ashley, W., Irizarry, A., & Hall, S. (2014). A climatology of Tornado intensity assessments. *Meteorological Applications*, *22*(3), 513–524. https://doi.org/10.1002/met.1482

Song, D. X., Huang, C., He, T., Feng, M., Li, A., Li, S., ... & Townshend, J. R. (2021). Very Rapid Forest Cover Change in Sichuan Province, China: 40 Years of Change Using Images From Declassified Spy Satellites and Landsat. IEEE Journal of Selected Topics in Applied Earth Observations and Remote Sensing, 14, 10964-10976.

United States Geological Survey (USGS). (2020). What are the band designations for the Landsat satellites? Retrieved April 15, 2022, from https://www.usgs.gov/faqs/what-are-band-designations-landsat-satellites?qt-news_science_products=0#qt-news_science_products

Womble, J. A., Wood, R. L., & Mohammadi, M. E. (2018). Multi-scale remote sensing of tornado effects. *Frontiers in Built Environment*, *4*. https://doi.org/10.3389/fbuil.2018.00066

Wurman, J., Kosiba, K., & Robinson, P. (2013). In situ, Doppler radar, and video observations of the interior structure of a tornado and the wind–damage relationship. Bulletin of the American Meteorological Society, 94(6), 835-846.